Original article with supplementary data

Epileptic Disord 2014; 16 (1): 31-44

Cortical network dysfunction in musicogenic epilepsy reflecting the role of snowballing emotional processes in seizure generation: an fMRI-EEG study

Volker Diekmann [1], Anselm Cornelius Hoppner [2]

[1] Sektion Neurophysiologie, Universität Ulm
[2] Abteilung Neurologie, RKU Ulm, Ulm, Germany

Received July 29, 2013; Accepted December 04, 2013

ABSTRACT – *Aim*. Patients suffering from musicogenic epilepsy have focal seizures triggered by auditory stimuli. In some of these patients, the emotions associated with the music appear to play a role in the process triggering the seizure, however, the significance of these emotions and the brain regions involved are unclear. In order to shed some light on this, we conducted fMRI and EEG in a case of musicogenic epilepsy. *Methods*. In a 32-year-old male patient with seizures induced by a specific piece of Russian music, we performed video-EEG monitoring as well as simultaneous fMRI and EEG registration. *Results*. Video-EEG monitoring revealed a left temporo-frontal epileptogenic focus. During fMRI-EEG co-registration, BOLD signal alterations were not only found in the epileptogenic focus but also in areas known for their role in the processing of emotions. Prior to a seizure in some of these areas, BOLD contrasts exponentially increased or decreased. *Conclusion*. These results suggest that in our case, dysfunction of the regulation processes of the musically-induced emotions, and not the musical stimulus itself, led to the seizures.

Key words: musicogenic epilepsy, fMRI, EEG, emotional process, exponential BOLD changes

Correspondence:
Anselm Cornelius Hoppner
Abteilung Neurologie,
RKU Ulm,
Abt. Neurologie,
Oberer Eselsberg 45,
D-89081 Ulm, Germany
<anselm.hoppner@uni-ulm.de>

doi:10.1684/epd.2014.0636

Musicogenic epilepsy is a very rare disease. Although it has been known for more than 75 years (Critchley, 1937), little is known about the underlying mechanism. In the past two decades, several cases have been reported in which clinical findings together with EEG and functional imaging (SPECT and fMRI) were used to try to understand the epileptogenesis in these patients (Wieser *et al*., 1997; Gelisse *et al*., 2003; Morocz *et al*., 2003; Marrosu *et al*., 2009). Earlier ictal SPECT-based findings (Gelisse *et al*., 2003) pointed towards changes in

metabolism in the temporal lobe, ipsilateral to the assumed focus. In another case, ictal fMRI showed an increase in BOLD signal in several regions including, not only the left temporal region ipsilateral to the assumed epileptogenic focus, but also the dorsal frontal areas and right temporal regions, the nucleus accumbens, insula, orbito-frontal regions, and anterior and occipital areas of the cingulum (Marrosu *et al*., 2009). In one case, BOLD signal increased in the ipsilateral temporal lobe, in acoustic areas of the right hemisphere, bifrontal areas, and surface of the brain, while decrease in BOLD signal was described in the right gyrus rectus, subcallosal gyri, and small areas in the orbital gyrus, bilaterally (Pittau *et al*., 2008). The respective seizure foci of these patients was located to the right fronto-temporal region. These findings led to the conclusion that the epileptogenic zone in these patients was in the right hemisphere. In another case, an increase in BOLD signal was reported in the left anterior temporal lobe, ipsilateral to the assumed epileptogenic focus (Morocz *et al*., 2003). In this case, as well as another already mentioned (Marrosu *et al*., 2009), changes in BOLD signal appeared in the assumed epileptogenic focus. The role of emotions in triggering seizures is occasionally mentioned in case reports (Wieser *et al*., 1997; Pittau *et al*., 2008), although in these cases it was even more enigmatic. The above-mentioned data suggest that in musicogenic epilepsies, miscellaneous areas are involved in triggering seizures including, not only the acoustic areas, but other cortical areas. In our own patient, seizures were triggered by a specific type of Russian music and were accompanied by a certain pleasant feeling. This led to the reasonable suspicion that emotion may play a role in this particular musicogenic epilepsy. Because the seizures in our patient could be reproducibly triggered by the appropriate musical stimulus, this case offered a chance to identify the cortical areas involved, with attention to areas contributing to cortical processing of acoustic stimuli and emotion.

Methods

Case study

A 32-year-old, right-handed male patient was referred to our video-EEG-monitoring unit by an external neurological practitioner. The patient reported seizures induced by listening to a certain type of music, which he referred to as "Chanson" (referred to here as "Russian Chanson" [RC]), which is popular in the ethnic group of Russian immigrants of German ancestry. He was able to understand the standard terms in which music is described (rhythm, motif, instrument, and voice), however, no specific stimulus could be identified. A first episode might have occurred when listening to music as a teenager, but at the time of the event he was unobserved and other episodes had not occurred until he suffered a first generalised tonic-clonic seizure (GTCS) at the age of 25 years, when he was found non-responsive (with a recovery time of about 20 minutes; a diagnosis was made although no tongue biting or enuresis was described). Since then, he experienced focal dyscognitive seizures when he was exposed to the above-mentioned music. The semiology of the focal dyscognitive seizures was described as follows: the music first induced a certain pleasant feeling, which then turned into a non-specific aura with an uncomfortable feeling, and a feeling "in his heart" that a seizure was about to happen. The focal dyscognitive seizure, which developed afterwards, was initiated by oral automatism, impaired consciousness with partial non-responsiveness, fluent sensomotor aphasia, and automatism of the right upper extremity resembling the act of conducting a musical orchestra. Enuresis, encopresis, or tongue biting, as sequelae of generalised tonic-clonic seizures, were not reported. The patient had been treated with carbamazepine at up to 900 mg per day and oxcarbazepine at 1,200 mg per day, with no effect.

Experimental procedures

Medication of the patient was stopped one week before admission to the video-EEG monitoring unit. Video-EEG monitoring was performed with electrodes placed according to the international 10-20 system, and video, ECG and blood pressure were co-registered. At the end of the monitoring procedure, the patient was exposed to a provoking stimulus five times using in-ear head-phones in order to expose him unilaterally to the stimulus, as well as *via* normal audio boxes at low volume.

After this clinical characterisation, an fMRI study with co-registration of electrophysiological signals was performed. The patient was equipped with high-quality electrostatic headphones and an optical microphone (NNL AudioSystem, NordicNeuroLab, Bergen, Norway) to ensure scanner noise reduction, sound stimulation, and communication with the patient. To avoid eye movements during acquisition of the functional data, the patient fixated on a cross presented *via* a MRI-compatible visual stimulation system (NNL VisualSystem, NordicNeuroLab, Bergen, Norway). We acquired electrophysiological signals and fMR images during three separate conditions: (i) without sound stimulus (duration: 417 seconds); (ii) while listening to pink noise (PN; duration 200 seconds) and Styrian folk music (SFM; duration: 186 seconds); and (iii) to

the above-mentioned RC (duration: 198 seconds). At 143 seconds after the beginning of the RC, the patient developed a GTCS and fMRI and electrophysiological acquisition was terminated. The SFM stimulus was chosen because it was, in musical terms, similar to the RC stimulus.
All procedures were approved by the local ethics board and performed after written consent was given by the patient.

MRI acquisition
Functional and anatomical images of the whole brain were acquired with a 1.5 T Siemens Symphony scanner using a standard cylindrical head coil for rf-signal emission and detection. For details of MRI acquisition characteristics, see the supplementary data section at the end of the paper.

MRI data processing
The functional MR images were preprocessed and analysed using the methods implemented in the SPM8 software package (Statistical parametric mapping, Wellcome Department of Imaging Neuroscience, London, UK) (Friston *et al*., 1995). Functional images were corrected for motion artefacts. The patient's functional data were co-registered with the anatomical scans and both were normalised to the Montreal Neurological Institute (MNI) standard space using the projection matrices of the cerebrospinal fluid (CSF). Grey and white matter segmented images were evaluated using the anatomical MP-RAGE image of the CSF and grey and white matter tissue probability maps implemented in SPM8. The normalised functional images were spatially smoothed with an 8-mm isotropic Gaussian kernel.

Statistical analysis of functional images
A general linear model was applied to the time series formed by the intensity of each voxel. The epochs with sound stimuli were modelled by box-car functions. To account for possible changes of mood with time, we implemented a second regressor, changing exponentially with time (*supplementary data: figures S1 and S2*). To gain additional flexibility in the analysis of BOLD changes over time, the session in which the seizure was provoked by the Russian song stimulus was divided into three epochs; 1, 2 and 3 (duration: 56.4, 53.58, and 53.58 seconds, respectively), each described by a box-car function as sound stimulus (S) and a regressor function increasing exponentially with time, as emotional regressor (E). The box-car functions named "pn_S" during the PN stimulus, "sfm_S" during the SFM stimulus, and "S1", "S2" and "S3" during the RC stimulus convolved with the canonical haemodynamic response function implemented in SPM8, and the exponential functions named "pn_E" during PN, "sfm_E" during SFM, and "E1", "E2" and "E3" during RC stimulation served as regressors of interest. Additionally, we used the realignment parameters computed in the motion correction pre-processing step as confounding head movement regressors of no interest. Slow technical and physiological fluctuations of the BOLD signal were suppressed by high-pass filtering (time constant: 81 seconds). To account for serial correlation between successive scans, the model's noise component was described as a first-order autoregressive process. The coefficients of all regressors were then estimated for each session using the restricted maximum likelihood estimation scheme implemented in SPM8 (fixed effects model). BOLD signal changes were assumed to be valid if the F- or t-values of clusters of at least 5 voxels exceeded a level corresponding to a corrected family wise error (FWE) *p*-value of 0.05.
Anatomical regions were identified by the "Anatomy" toolbox of SPM8 (Eickhoff *et al*., 2005) and the "WFUPickatlas" toolbox of SPM8 (Maldjian *et al*., 2003).

EEG acquisition
EEG, ECG, and horizontal and vertical EOG signals, using a 16-channel EEG amplifier system constructed and built in our laboratory (see supplementary data), were simultaneously recorded along with the functional images. Ring-type Ag-AgCl EEG electrodes with integrated 12-kΩ protection resistors (Easycap GmbH, Herrsching, Germany) were placed according to the 10-20 system and referenced to a common electrode placed at FCz. The artefacts in the electrophysiological signals induced by the MR gradient switching, the vacuum pump of the scanner, and the pulse artefacts within the bore of the magnet were largely eliminated by a software package developed in our laboratory.

Results

Video-EEG monitoring
Spikes with a maximum over T1, T7 and F1 with a frequency of 10/hour, as well as theta activity temporally on the left side, were recorded interictally. Exposure of the left ear to the Russian music for 64 seconds, as well as exposure to both ears at low volume, led to a typical aura, followed by a focal dyscognitive seizure with oral automatisms, impaired consciousness, aphasia, and motor signs of the right upper extremity after one second. EEG showed spike waves with a maximum over the left temporal electrodes. Exposure to the right ear for three minutes did not lead to a seizure or changes in the EEG during video-EEG monitoring, but led to changes based on fMRI-EEG co-registration. At the end of the first documented seizure, the patient

grasped his nose with his left hand, which was interpreted as a lateralisation sign for a left-hemispheric focus.

fMRI

No significant differences were found between SFM and pink noise or between the sound stimuli regressors S1, S2 and S3 of the three epochs during stimulation with the RC. In contrast, there were significant differences between the patient's functional MR BOLD responses during the RC stimulation as well as similar differences relative to SFM or pink noise. In the following, we will focus on the results obtained with RC stimulation and the differences between RC and SFM stimulation, as the SFM is much more similar to the RC than pink noise.

In many areas, significantly *greater* BOLD responses were indicated by the contrasts between the stimulus regressors S1, S2 and S3 and the SFM stimulus regressor sfm_S (*supplementary data: table S1*). However, the number of significant clusters and voxels decreased continuously from the first (S1), over the second (S2), to the last (S3) epoch. In the first epoch (*figure 1a*), we found significant bilateral clusters in the cerebellum, prefrontal and orbito-frontal cortex, left hemispheric dorso-lateral frontal and parietal cortex, left entorhinal and cornu Ammonis hippocampal areas, the left amygdala and right parieto-temporal cortex, and the right supplementary motor area (SMA) with a dominance in the left hemisphere (380 *versus* 172 voxels). Most of the significant cerebellar, hippocampal and amygdala, temporal and parietal, and SMA voxels already disappeared in the second epoch and only a few left-sided cerebellar cortical voxels and bilateral orbito-frontal voxels persisted in the last epoch, just before the seizure started (*supplementary data: table S1)*.

The contrasts sfm_S-S1>0, sfm_S-S2>0, and sfm_S-S3>0 also revealed significant BOLD *decreases* between RC and sfm_S stimulation, with clear dominance in the right hemisphere (174 voxels on the left and 384 voxels on the right; *supplementary data: table S2*). Stimulus-related BOLD decreases changed little from the first (*figure 1b*) to the second RC epoch, whereas the number of significant clusters and voxels was reduced in the last (S3) epoch. All three RC stimulus regressors revealed BOLD reduction with respect to SFM in the following regions: the right temporal pole, right cerebellum, right orbito-frontal cortex, bilateral visual cortex, left and right (more pronounced) ventral prefrontal cortex, right dorsal prefrontal cortex, and the pre- and post-central gyri. Regressors S1 and S2 also showed BOLD decreases in right parietal cortex and regressors S1 and S3 in left orbito-frontal areas. Further reductions were observed in the anterior cingulate cortex during S1, the right amygdala and left cerebellar areas during S2, and the left orbito-frontal cortex during S3.

The regressors with exponential rise yielded no significant BOLD changes in any of the stimulus epochs except E3, the epoch prior to the seizure onset (*table 1*). In this epoch, significant BOLD activations were found in two large clusters and a number of smaller clusters (*figure 2*). One large cluster comprised bilateral regions in Brodmann Area 6 (200 voxels; left superior and middle frontal gyri and bilateral SMA) and the other was in the left cerebellum (198 voxels). Smaller significant clusters were found on the right and more pronounced in the left entorhinal hippocampal areas, at two sites in the right cerebellum, right visual cortex areas (V3v, V4); and the right medial temporal pole.

Masking the E3>0 contrasts by the contrast S1>0 (data not shown) (*table 1*) exhibited some overlap with the BOLD activation related to S1 but most of the BOLD signal revealed by the E3 regressor occurred in areas outside those indicated by S1 or S2. This means that the significant E3 regressor values did not simply represent a shift from the physical stimulus regressor signal change (formerly represented by the S1 and S2 regressors in epoch 1 and 2) to an exponentially increasing signal change (represented by the E3 regressor in epoch 3), but reflect a process in its own right.

Parallel to the BOLD signal increases, the E3 regressor also revealed large regions where BOLD signal *reductions* significantly increased exponentially with time (*table 2*). Similar to the right hemispheric dominance of BOLD decreases found in the physical stimulus contrasts S1<sfm_S, S2<sfm_S, and S3<sfm_S, the right hemispheric E3<0 contrast was greater in the right side (1,768 voxels on the right *versus* 862 voxels on the left). Exponential BOLD decreases occurred bilaterally in the frontal and orbito-frontal cortex, superior and inferior parietal lobule, cuneus and precuneus, and left anterior cingulate. Smaller clusters with significant exponential BOLD decreases were found in the left and right Broca areas (BA44/45) and in the left temporal cortex.

Similar to the observed increased BOLD signal contrast E3>0, the E3<0 contrast masked by the S1<0 contrast demonstrated that most of the significant exponentially decreasing BOLD signal voxels did not overlap with stimulus-related deactivation during epoch 1, *i.e.* they represented BOLD changes in areas exclusively found in epoch 3.

EEG

Without sound stimulation and during the pink noise stimulation, no epileptogenic patterns were found. At the end of the SFM epoch, two spike wave patterns could be identified in the left fronto-temporal

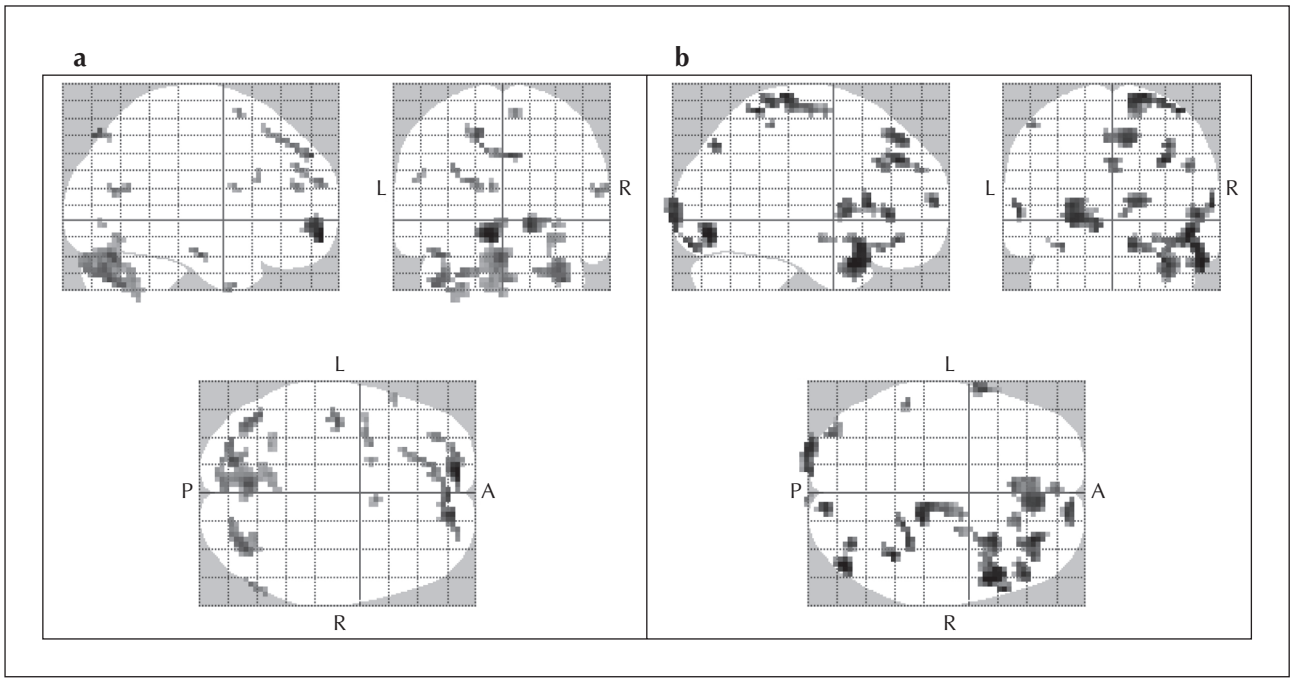

Figure 1. Maximum intensity projection of significant BOLD contrast values of the first epoch of RC stimulation regressor S1 *versus* SFM stimulation regressor S_sfm. Results of t-test, significance levels ($p \leq 0.05$) family-wise error corrected, and cluster size ≥5 voxels. (a) S1>S_sfm showed dominance of left hemispheric BOLD signal increases (380 voxels on the left *versus* 172 voxels on the right). (b) S1<S_sfm demonstrated clear dominance of right hemispheric BOLD signal reductions (174 voxels on the left and 382 voxels on the right).
L: Left; R: right; A: anterior; P: posterior.

leads (F7, T3). During the RC stimulation, the patient showed nine spikes or spike-wave patterns prior to the seizure which were visible in both hemispheres at the fronto-temporal, frontal, and central leads. At 143 seconds after the beginning of the RC, a focal dyscognitive seizure initiated (*figure 3*) with successive generalisation. Because of the strong movement artefacts within the bore of the MRI machine, accompanying the patient's seizure, the electrographic seizure potentials could not be reconstructed.

Discussion

We conducted a fMRI study of a patient with musicogenic epilepsy, whose seizures could be triggered by a specific type of Russian music, but not by similar music of different origin. A distinct lateralisation of the triggering stimulus, as reported by Gelisse *et al*. (2003), could not be observed, as seizures were triggered while listening to appropriate stimulus unilaterally on either side. While the patient's clinical signs (aphasia), as well as his EEG data, point to a left hemispheric fronto-temporal epileptogenic focus, BOLD activity during stimulation by the seizure-provoking music was also observed in many other areas.

Affective stimulus processing

By dividing the stimulation period into three epochs, S1, S2 and S3, we found that the RC initially (epoch S1) induced increased BOLD activity in the left amygdala, left hippocampal areas, left dorso-medial prefrontal cortex (BA9/10), left-sided Broca areas (BA44/45), right-sided temporo-parietal junction area (BA39), and right premotor cortex (BA6). These regions are known to be part of the affective emotional network, with right BA39 and BA6 being particularly involved in positive stimuli processing. Additionally, two cerebellar clusters (right lobule VI and left lobules VIIb, VIIIa and b) showed increased BOLD signal in epoch 1 of the RC stimulation. It is widely accepted by now that the cerebellum is not only concerned with motor control, but is also involved in emotional processing (Baumann and Mattingley, 2012). Thus, the BOLD signal increases observed during S1 are likely to reflect various aspects of the affective stimulus processing of the RC.

Emotional processing

During the following epochs, much of the BOLD increases observed during epoch 1 disappeared, whereas most BOLD signal decreases persisted during

Table 1. BOLD contrast RC exponential regressor E3 > 0. Exponentially *increasing* BOLD changes E3>0 during last epoch of RC stimulation. Masking of the significant E3>0 voxels by the BOLD response map S1>0 ($p \leq 0.05$ family wise error corrected, cluster size ≥5) demonstrated that most of the BOLD signal revealed by the E3 regressor occurred in areas outside those indicated by the S1 regressor (exclusively masked columns). Results of t-test, significance levels $p \leq 0.05$ family wise error corrected, cluster size ≥5 voxels.

Region	Brodmann area/sub-region	left (L)/ right (R)	unmasked				masked exclusive S1>0			
			MNI co-ordinates (mm)			nVOX	MNI co-ordinates (mm)			*n*VOX
			x	y	z		x	y	z	
Hippocampus, Fusiform Gyrus	EC	L	-30	2	-44	35	-27	-1	-41	17
Hippocampus, Inferior Temporal Gyrus	EC	R	30	2	-41	5	30	2	-41	4
Cerebellum	VIIIa, b (Vermis)	R	0	-73	-38	9				
Cerebellum	I-VI (Hem)	R	30	-31	-38	14	30	-31	-38	14
Medial Temporal Pole	n.a.	R	39	14	-38	15	39	14	-38	15
Inferior Temporal Gyrus (Probably Wm)	n.a.	R	45	-10	-29	11	45	-10	-29	11
Cerebellum	VI, VIIa Crus I, II	L	0	-65	-20	196				
Cerebellum	VI, VIIa Crus I	R	30	-85	-17	38	30	-85	-17	30
Inferior Occipital Gyrus (Probably Wm)	n.a.	L	-30	-94	-5	11	-30	-94	-5	11
Inferior Occipital Gyrus	BA17, BA18, V3v, V4v	R	27	-94	1	26	27	-94	1	26
Middle Frontal Gyrus (Probably Wm)	n.a.	R	33	11	55	6	33	11	55	6
Superior Frontal Gyrus, Middle Frontal Gyrus, Supplementary Motor Area	BA6	L, R	-24	-16	64	200	-24	-16	64	181

MNI: Montreal Neurological Institute; *n*VOX: number of voxels; n.a.: not available.

the following two epochs, although with reduced extension. As a noticeable exception, during S2, an augmented deactivation was observed in the right ventro-lateral pre-frontal cortex (BA 45) and a new area of decrease emerged in the right amygdala. Interestingly, Goldin *et al*. (2008) and Dolcos *et al*. (2011) reported that a cognitive reappraisal of negative emotions was associated with a BOLD decrease in these areas. Thus, the pattern observed during S2 might reflect an increasing dominance of cognitive control over affective neural processes. With respect to the preictal events in our patient, the last 54 seconds of the RC stimulation prior to the seizure (epoch 3) clearly represented the most interesting and intriguing epoch. The BOLD signal of this epoch fit best with an exponentially changing regressor and, therefore, is likely to reflect neural events with an exponential time course. Of particular interest are those areas where the exponential activation engulfed larger volumes than outlined by the stimulus-driven regressor in S1 and/or where it emerged *de novo* during S3. Hippocampal entorhinal cortex was one

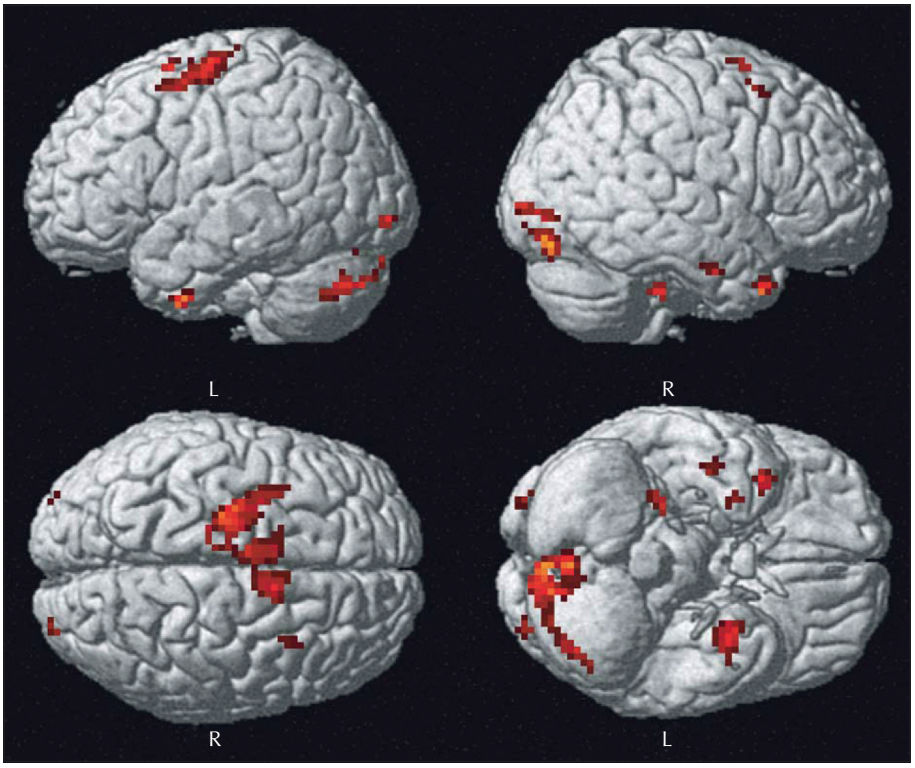

Figure 2. Map of significant snowballing BOLD increases during the last epoch of RC stimulation. Results of t-test E3>0, significance levels ($p \leq 0.05$) family-wise error corrected, and cluster size ≥5 voxels projected on the single subject rendered brain of SPM8.

such area. As this area appears to be specifically engaged in the encoding of emotional material (Dolcos *et al*., 2004), its bilateral exponential activation may be related to the patient's growing episodic memory activity induced by the RC stimulus. Another such area was the right temporal pole, a structure which has been implied in the evaluation of affective emotions (Mathiak *et al*., 2011). More specifically, Kret *et al*. (2011) found the right temporal pole to belong to a network which is positively correlated with the emotional feeling of social inhibition and the activation of which, in the present case, might reflect a melancholic feeling triggered by the RC. The largest cluster of significantly increasing BOLD activity that had no overlap with the stimulus driven activity of epoch 1 was located in the bilateral SMA and left hemispheric Brodmann area 6. Ochsner *et al*. (2002) and Goldin *et al*. (2008) found that these areas showed increased BOLD signals in early cognitive processes for the regulation of emotion. This lead to the reasonable suspicion that processes of cognitive emotion regulation in our patient snowballed prior to the seizure, and pointed to a dysfunction in the emotion regulation network which finally triggered the seizure. Moreover, in a case study of reading epilepsy, Vaudano *et al*. (2012) observed a BOLD increase prior to seizure onset in bilateral SMA and left hemispheric lateral BA6 pre-motor area, at locations very similar to those of our patient. According to these authors, BA6 could have been an area linking cognitive activation and seizure activity in their patient. The broad pre-frontal, frontal, orbito-frontal, and parietal areas which showed increasing loss of BOLD signal during epoch 3 of the RC stimulation, may be a hint that the activity was increasingly reduced in brain areas known to be involved in sensory and speech processing. Given that this area also subserves cognitive control tasks (Dolcos *et al*., 2011), its deactivation, in contrast to the activation of left BA6, might indicate that these areas address different aspects of emotion.

Overall remarks

In summary, although many details of the above interpretation are necessarily speculative in view of the single case presented in this study, we hold that, taken together, the observed pattern of BOLD activity supports the notion that an "exploding" activity in emotion-related areas dominated the period immediately preceding seizure onset. The scarce case reports on musicogenic epilepsy characterise the seizure evoking stimulus mostly in musical terms (overview in Pittau *et al*. [2008]), and imply the primary

Table 2. BOLD contrast RC exponential regressor E3<0. Exponentially *decreasing* BOLD changes E3<0 during last epoch of RC stimulation. Masking of the significant E3<0 voxels by the BOLD response map S1<0 ($p \leq 0.05$ family wise error corrected, cluster size ≥5) demonstrated that most of the BOLD signal revealed by the E3 regressor occurred in areas outside those indicated by the S1 regressor (exclusively masked columns). Results of t-test, significance levels $p \leq 0.05$ family wise error corrected, cluster size ≥5 voxels.

Region	Brodmann area/sub-region	left (L)/ right (R)	unmasked				masked exclusive S1>0			
			MNI co-ordinates (mm)			*n*VOX	MNI co-ordinates (mm)			nVOX
			x	y	z		x	y	z	
Cerebellum	VIIa Crus 1	L	-36	-85	-17	6				
Cerebellum	VIIa Crus 1	R	12	-91	-17	9				
Superior Orbital Gyrus, Inferior Frontal Gyrus (P. Orbitalis)	BA10, 11 BA44, 45	L, R	12	44	-14	1724	33	41	-11	1492
Middle Temporal Gyrus	n.a.	L	-60	2	-11	7	-60	2	-11	7
Temporal Pole	n.a.	L	-42	17	-11	17	-42	17	-11	17
Inferior Frontal Gyrus, Inferior Frontal Gyrius (P. Orbitalis)	BA45	L	-57	20	4	44	-57	20	4	44
Rolandic Operculum, Inferior Frontal Gyrus (P. Opercularis)	BA44, BA45	R	63	5	19	21	63	5	19	21
Middle Occipital Gyrus, Inferior Parietal Cortex	PGp	R	45	-82	22	8	45	-82	22	8
Superior Occipital Gyrus	BA18	R	18	-97	25	9	18	-97	25	9
Anterior Cingulate, Superior Medial Gyrus	BA32, 33	L, R	0	26	34	98	0	23	37	69
Superior Parietal Lobule, Inferior Parietal Lobule, Cuneus, Superior Occipital Gyrus	BA7A, BA18, PGp	L, R	-33	-79	46	479	-33	-79	46	479
Post-Central Gyrus, Superior Parietal Lobule, Precuneus, Middle Occipital Gyrus	BA1, 2, 3b, 4p, BA7A, 7M, 7PC, PGp	R	21	-43	57	492	18	-46	67	435
Precentral Gyrus	BA4a, p, BA6	R	15	-31	70	7				

MNI: Montreal Neurological Institute; *n*VOX: number of voxels; n.a.: not available.

auditory cortex in epileptogenesis. Therefore, a relationship between the high structural organisation of the auditory cortex and the propensity to develop seizures upon musical stimulation was suggested (Gelisse *et al*., 2003). In our patient, the musical characteristics *per se* do not appear to be the crucial factor evoking the epileptic seizure. For one thing, the traditional Styrian tune, with musical characteristics very similar to the epileptogenic Russian song, did not lead to seizures in our patient and, unlike the Russian song, did not engender exponential BOLD signal changes. Moreover, these changes did not occur in the primary

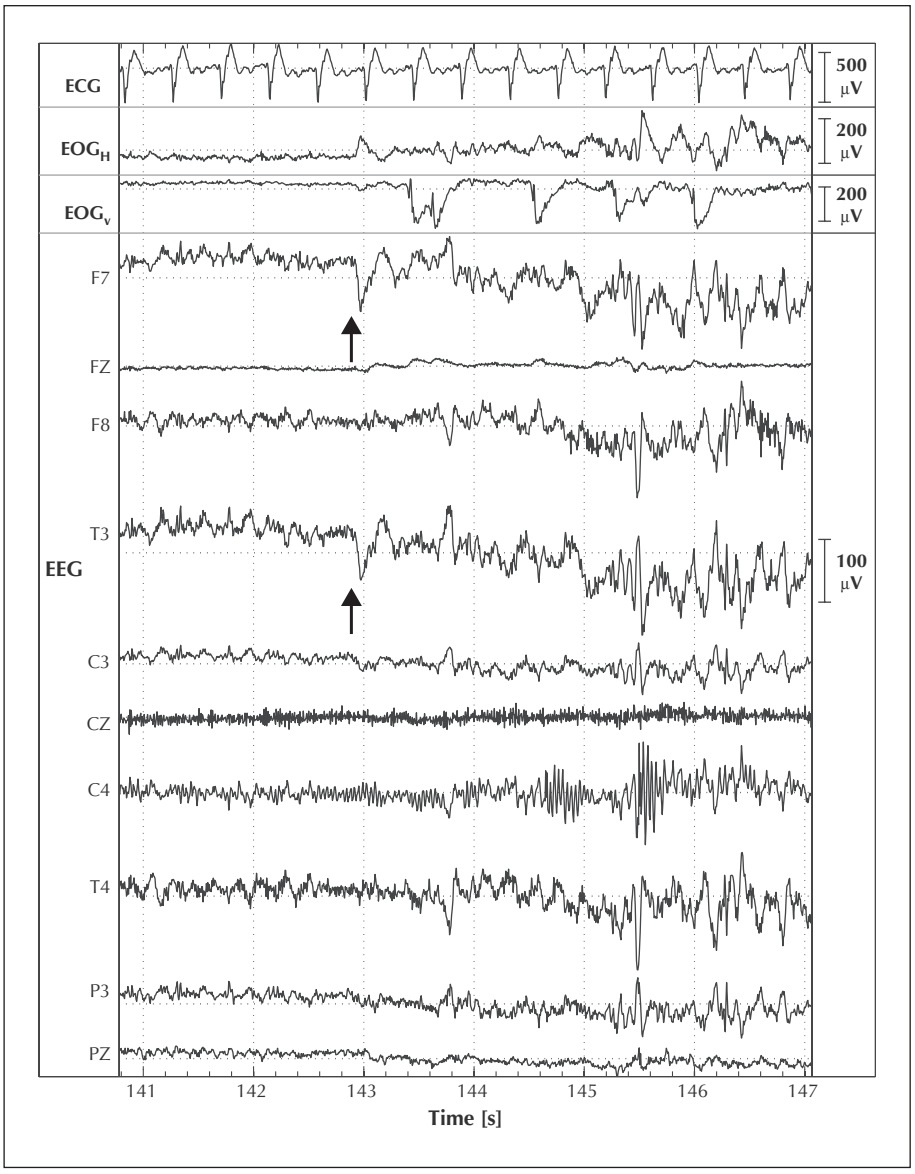

Figure 3. ECG, EOG, and EEG data plot co-registered with fMRI acquisition.
Time scale is relative to the beginning of the RC stimulation. Black arrows at ≈143 seconds mark the start of the seizure, as observed at leads F7 and T3. Plot shows data after software reduction of MR gradient switching, pulse wave and vacuum pump noise, and filtered by a 163-Hz 40 dB/octave finite impulse response digital low-pass filter. ECG thorax lead registration, $EOG_{H, V}$ horizontal and vertical EOG, and EEG electrode positions according to the 10-20 system were referenced to an electrode at position FCz.

auditory cortex but in areas supposedly related to cognitive processing and regulation of emotions. Thus, we surmise that it is either the emotion (perhaps a specific form of melancholy) created by the *combination* of melody and native language which ultimately sparked our patient's epileptic activity, or, alternatively, in view of the activity in areas related to the control of emotion, the attempt to confine this emotion. To further test this notion, one could have presented the Russian song in a different language or with the Russian lyrics adapted to a Western melody, or other combinations. However, to avoid the danger of secondary generalisation of the patient's seizures, we refrained from such tests. In summary, the available results, in particular the locations of BOLD activity which correlated with "snowballing" regressors, suggest that dysfunction of networks involved in processing and regulating emotions, induced by a specific combination of melody and lyrics, played a major role in ictogenesis in our patient. □

Acknowledgments and disclosures.
We thank Wolfgang Becker for critical reading of the manuscript, Wolfgang Becker and Frank Kerling for fruitful discussions, and Ralph Kühne for technical assistance.
None of the authors have any conflict of interest to disclose.

References

Baumann O, Mattingley JB. Functional topography of primary emotion processing in the human cerebellum. *Neuroimage* 2012; 61: 805-11.

Critchley M. Musicogenic epilepsy. *Brain* 1937; 6013-27.

Dolcos F, LaBar KS, Cabeza R. Interaction between the amygdala and the medial temporal lobe memory system predicts better memory for emotional events. *Neuron* 2004; 42: 855-63.

Dolcos F, Iordan AD, Dolcos S. Neural correlates of emotion-cognition interactions: a review of evidence from brain imaging investigations. *J Cogn Psychol (Hove)* 2011; 23: 669-94.

Eickhoff SB, Stephan KE, Mohlberg H, *et al*. a new SPM toolbox for combining probabilistic cytoarchitectonic maps and functional imaging data. *Neuroimage* 2005; 25: 1325-35.

Friston K, Holmes A, Worsley K, Poline J, Frith C, Frackowiak R. Statistical parametric maps in functional imaging: a general linear approach. *Hum Brain Mapp* 1995; 2: 189-210.

Gelisse P, Thomas P, Padovani R, Hassan-Sebbag N, Pasquier J, Genton P. Ictal SPECT in a case of pure musicogenic epilepsy. *Epileptic Disord* 2003; 5: 133-7.

Goldin PR, McRae K, Ramel W, Gross JJ. The neural bases of emotion regulation: reappraisal and suppression of negative emotion. *Biol Psychiatry* 2008; 63: 577-86.

Kret ME, Denollet J, Grezes J, de Gelder B. The role of negative affectivity and social inhibition in perceiving social threat: an fMRI study. *Neuropsychologia* 2011; 49: 1187-93.

Maldjian JA, Laurienti PJ, Kraft RA, Burdette JH. An automated method for neuroanatomic and cytoarchitectonic atlas-based interrogation of fMRI data sets. *Neuroimage* 2003; 19: 1233-9.

Marrosu F, Barberini L, Puligheddu M, *et al*. Combined EEG/fMRI recording in musicogenic epilepsy. *Epilepsy Res* 2009; 84: 77-81.

Mathiak KA, Klasen M, Weber R, Ackermann H, Shergill SS, Mathiak K. Reward system and temporal pole contributions to affective evaluation during a first person shooter video game. *BMC Neurosci* 2011; 12: 66.

Morocz IA, Karni A, Haut S, Lantos G, Liu G. fMRI of triggerable aurae in musicogenic epilepsy. *Neurology* 2003; 60: 705-9.

Ochsner KN, Bunge SA, Gross JJ, Gabrieli JD. Rethinking feelings: an fMRI study of the cognitive regulation of emotion. *J Cogn Neurosci* 2002; 14: 1215-29.

Pittau F, Tinuper P, Bisulli F, *et al*. Videopolygraphic and functional MRI study of musicogenic epilepsy. A case report and literature review. *Epilepsy Behav* 2008; 13: 685-92.

Vaudano AE, Carmichael DW, Salek-Haddadi A, *et al*. Networks involved in seizure initiation. A reading epilepsy case studied with EEG-fMRI and MEG. *Neurology* 2012; 79: 249-53.

Wieser HG, Hungerbuhler H, Siegel AM, Buck A. Musicogenic epilepsy: review of the literature and case report with ictal single photon emission computed tomography. *Epilepsia* 1997; 38: 200-7.

Supplementary data

Methods

MRI characteristics

Functional image characteristics: T2* gradient echo-planar sequences of axial slices parallel to the APline; slice thickness: 3.5 mm; gap: 0.5 mm; in-plane resolution: 3.59×3.59 mm^2, $64 \times 64 \times 32$ voxels; repetition time, TR: 2,820 ms; echo time, TE: 50 ms; and flip angle, FA: 90°. Anatomical image characteristics: (1) 3-D sequence (magnetization prepared rapid gradient echo, MP-RAGE) $256 \times 256 \times 256$ voxels of $0.98 \times 0.98 \times 1$ mm^3; TR: 1,740 ms; TE: 2.8 ms; inversion recovery time, TI: 880 ms; FA=15°. (2) T2-weighted axial slice analogues of the functional images; slice thickness: 3.5 mm; gap: 0.5 mm; in-plane resolution: 0.45×0.45 mm^2, $512 \times 512 \times 32$ voxels; TR: 6,350 ms; TE: 99 ms; and FA: 150°.

EEG acquisition

The EEG system was controlled using a personal computer (PC) *via* an optical Ethernet connection which also transferred the digitilised data from the EEG machine to the PC. Each electrophysiological data channel was sampled with a time interval of 48 μs. The analogue to digital converters of the EEG amplifier system had an effective resolution of 19 bit (24 bit raw) which is equivalent to a resolution of approximately 0.4 μV. The high resolution in time and signal amplitude enabled potent reduction of MR gradient switching and other artefacts by software.

fMRI modelling

In *figure S1,* the regressors of sub-epoch 3, as an example of the model regressors of interest, were plotted.

Results

fMRI analysis

The fit in *figure S2* demonstrates that, in our opinion, it is justified to describe the BOLD data, in the epoch prior to and at the beginning of the seizure, by an exponential. In *tables S1 and S2,* the results of detailed BOLD analysis demonstrating differences between stimulus with RC and SFM are presented.

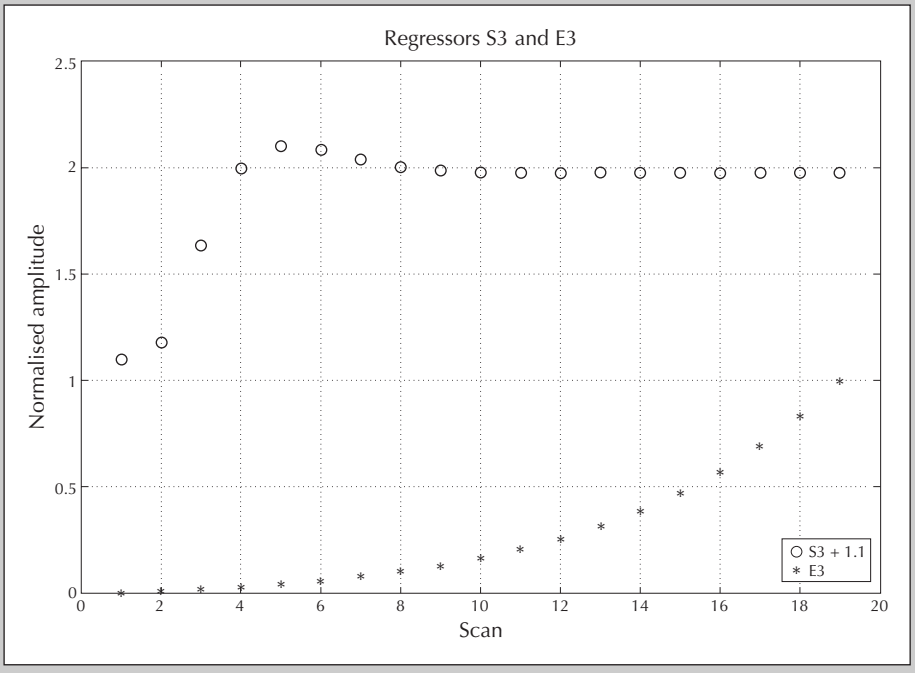

Figure S1. Regressors of interest of the general linear fMRI model of the last of the three epochs during RC stimulation. S3 (circles) normalised amplitudes as a function of MRI scan number of the regressor representing the acoustical stimulus convolved by the haemodynamic response function as implemented in SPM8, E3 (stars) normalised amplitude of the exponentially changing regressor.

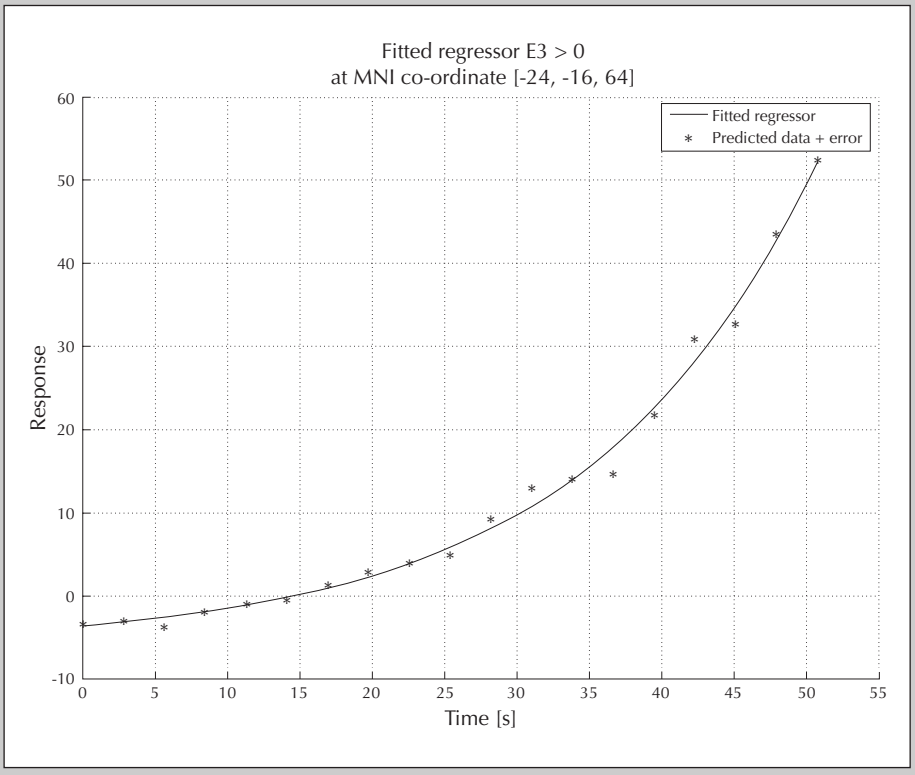

Figure S2. Results of the fitted fMRI model regressor E3>0 (black line) and the sum of the residual error and the data predicted by this regressor (stars). The fit represents the data of a voxel in Brodmann area 6 of the largest cluster with significant exponential BOLD increases during the last epoch of the RC stimulation.
Time scale is relative to the beginning of epoch 3. MNI (Montreal Neurological Institute) co-ordinates in mm.

Table S1. BOLD contrast RC stimulus > SFM stimulus.

Region	Brodmann area/sub-region	left (L)/ right (R)	MNI co-ordinates (mm)			S1	S2	S3
			x	y	z	*n*VOX	*n*VOX	*n*VOX
Cerebellum	VIIb (Hem), VIIIa (Hem), VIIIb (Hem)	L	-27	-58	-44	18		
Cerebellum	VIIa Crus I , Crus II (Hem)	L	-42	-67	-41	35	7	
Hippocampus	EC	L	-27	5	-41	13		
Cerebellum	VIIa Crus I (Hem), VIIa Crus II (Hem)	R	36	-73	-38	57	18	
Cerebellum	VI (Hem), VIIa Crus II (Hem), VIIa Crus II (Hem), IX (Hem)	L	-3	-70	-26	194	34	5
Inferior Temporal Gyrus, Hippocampus Amygdala	CA; LB	L	-42	-16	-23	12		
Cerebellum	VI	R	30	-67	-14	18		
Superior Orbital Gyrus	BA11	L	-9	59	-11	48	31	10
Medial Orbital Gyrus	BA10,11	R	15	56	-5	37	13	10
Fusiform Gyrus (Probably Wm)	n.a.	R	33	-76	-5	5	5	
Superior Frontal Gyrus	BA10	L	-21	59	22	15		
Middle Temporal Gyrus, Inferior Parietal Cortex	BA39	R	57	-70	16	14		
Probably Wm	n-a.	L	-18	5	19	6		
Superior Medial Gyrus	BA32	L	-9	44	19	8		
Inferior Frontal Gyrus (P. Triangularis)	BA44, 45	L	-57	20	22	7		
Middle Frontal Gyrus	BA9,10	L	-30	47	28	9		
Superior Medial Gyrus, Superior Frontal Gyrus, Middle Frontal Gyrus	BA9	R	3	43	37	32	16	
Superior Parietal Lobule, Inferior Parietal Lobule, Superior Occipital Gyrus	BA7A,P, PGa	L	-18	-82	49	15	5	
Supplementary Motor Area	BA6	R	6	8	64	9		

MNI: Montreal Neurological Institute; *n*VOX: number of voxels; S1 epoch: 0-56.4 seconds; S2 epoch: 56.4-109.8 seconds; S3 epoch: 109.8-163.4 seconds; n.a.: not available.

Table S2. BOLD contrast RC stimulus < SFM stimulus.

Region	Brodmann area/sub-region	left (L)/ right (R)	MNI co-ordinates (mm)			S1	S2	S3
			x	y	z	*n*VOX	*n*VOX	*n*VOX
Temporal Pole, Medial Temporal Pole	n.a.	R	54	11	-29	82	87	21
Temporal Pole	n.a.	R	30	14	-26	51	54	46
Superior Orbital Gyrus	BA11	R	18	29	-20	11		
Cerebellum	VI (Hem), VIIa Crus I (Hem)	R	12	-91	-17	15	10	7
Cerebellum	VI (Hem), VIIa Crus I (Hem)	L	-33	-88	-17		7	
Inferior Frontal Gyrus (P. Orbitalis)	BA11	R	39	38	-14	23	18	12
Amygdala	SF, LB	R	24	-10	-14		15	
Inferior Occipital Gyrus	V4v	R	45	-79	-11	30	18	8
Inferior Occipital Gyrus, Middle Occipital Gyrus, Calcarine Gyrus	BA17, 18, V3v	L	-27	-100	-2	72	53	9
Inferior Frontal Gyrus (P. Orbitalis)	BA45	R	51	32	1	27	50	23
Rolandic Operculum, Superior Temporal Gyrus	BA44, 45	L	-60	8	4	20	13	6
Inferior Frontal Gyrus (P. Triangularis)	BA45	R	60	20	7	14		9
Superior Medial Gyrus	BA9	R	15	49	10	25	18	16
Superior Medial Gyrus	BA9,10	L	0	53	28			5
Inferior Frontal Gyrus (P. Triangularis)	BA45	R	45	29	31	12	16	
Anterior Cingulate Cortex	BA32	L	-3	26	34	11		
Middle Frontal Gyrus	BA10	R	30	38	34	29	28	14
Middle Occipital Gyrus, Inferior Parietal Cortex (probably Wm)	PGp	R	33	-76	45	13	16	
Superior Medial Gyrus	BA9	L	-6	38	46	71	49	
Superior Parietal Lobule	BA1, 2, BA7A, 7PC	R	38	-49	64	12		5
Post-Central Gyrus (probably Wm)	BA3b, 4a, BA4b, 5L	R	33	-40	67	22	13	14
Precentral Gyrus, Supplementary Motor Area (probably Wm)	BA4a, 6	R	18	-31	73	16	29	8

MNI: Montreal Neurological Institute; *n*VOX: number of voxels; S1 epoch: 0-56.4 seconds; S2 epoch: 56.4-109.8 seconds; S3 epoch: 109.8-163.4 seconds; n.a.: not available.